

Superdeformation and alpha - cluster structure in ^{35}Cl

Abhijit Bisoi,¹ M. Saha Sarkar,^{1,*} S. Sarkar,² S. Ray,¹ M. Roy Basu,³ Debasmita Kanjilal,¹ Somnath Nag,⁴ K. Selva Kumar,⁴ A. Goswami,¹ N. Madhavan,⁵ S. Muralithar,⁵ and R. K. Bhowmik⁵

¹Saha Institute of Nuclear Physics, Bidhannagar, Kolkata - 700064, INDIA

²Bengal Engineering and Science University, Shibpur, Howrah - 711103, INDIA

³University of Calcutta, Kolkata - 700009, INDIA

⁴Indian Institute of Technology, Kharagpur-721302, INDIA

⁵Inter University Accelerator Centre, New Delhi - 110067, INDIA

(Dated: November 1, 2018)

A superdeformed (SD) band has been identified in a non - alpha - conjugate nucleus ^{35}Cl . It crosses the negative parity ground band above $11/2^-$ and becomes the yrast at $15/2^-$. Lifetimes of all relevant states have been measured to follow the evolution of collectivity. Enhanced $B(E2)$, $B(E1)$ values as well as energetics provide evidences for superdeformation and existence of parity doublet cluster structure in an odd-A nucleus for the first time in $A \simeq 40$ region. Large scale shell model calculations assign $(sd)^{16}(pf)^3$ as the origin of these states. Calculated spectroscopic factors correlate the SD states in ^{35}Cl to those in ^{36}Ar .

PACS numbers: 21.10.Re, 21.10.Tg, 21.60.Cs, 27.30.+t

The superdeformed bands observed in the even-even nuclei in upper sd shell have provided favourable condition to describe the collective rotation microscopically involving the cross-shell correlations [1, 2]. Complementary descriptions in terms of particle-hole excitations in the shell model [2, 3], and α -clustering configurations within various cluster models [4–6] have been utilised to interpret the data. Till now no such band has been observed in non - alpha - conjugate odd-A, $N \neq Z$ isotopes in this region [7]. If a nucleus clusterizes into fragments of different charge to mass ratios, the center of mass does not coincide with its center of charge. As a result a sizeable static E1 moment may arise in the intrinsic frame [8], resulting in several distinctive features in the spectra. Two adjacent opposite parity deformed $\Delta I = 2$ bands connected by strong E2 intra-band transitions in turn are connected by strong E1 inter-band transitions [8] forming an apparent $\Delta I = 1$ rotational band with alternating parity states. Since early seventies [9–11], a number of similar alpha-cluster bands have been studied extensively. In the spectrum of ^{19}F , cluster-model calculations have shown that coupling of a proton hole in the p shell coupled with four nucleons in the sd shell (a proton hole coupled to ^{20}Ne) gives rise to alpha-cluster bands. The lowest alpha + ^{15}N parity partner bands built on $K^\pi = 1/2^+$ ground-state band, lowest lying famous $K^\pi = 1/2^-$ at 110 keV and some other bands lying above 5 MeV have been observed. So far no similar clustering have been observed in odd A nuclei in the $A \simeq 40$ region, where evidences of clustering have been manifested in even-even nuclei through superdeformation.

According to Ikeda [12], in the spectra of light nuclei, cluster like configurations would appear near the threshold energy needed for breakup into proper sub-nuclei. For the nucleus of our interest ^{35}Cl , the threshold energy [13] to appear as a composite of ^{32}S and a triton (t) ($^{32}\text{S} + t$)

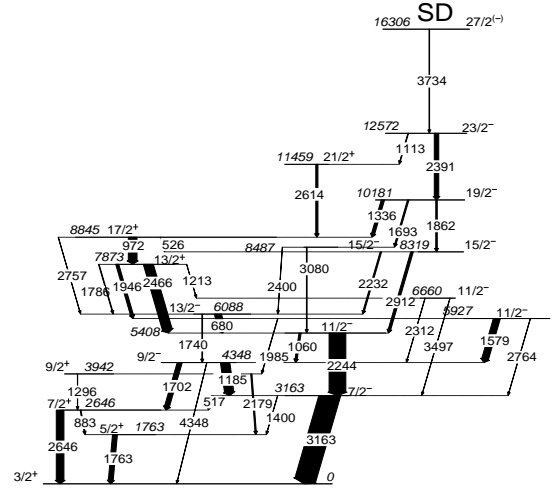


FIG. 1: Partial level scheme of ^{35}Cl .

is around 18 MeV. On the other hand, threshold for the decay of the composite system ^{35}Cl into $(^{31}\text{P} + \alpha)$ clusters is around 6.5 MeV. The SD rotational band observed in ^{36}Ar has been shown to have cluster structure. So one may expect to find deformed cluster bands in the excitation spectra of ^{35}Cl also generated by coupling a proton hole to SD states in ^{36}Ar .

In this letter, we report the observation of a superdeformed band for the first time in the odd A ^{35}Cl isotope. The reduced transition probabilities for all relevant transitions depopulating the states of the yrast negative parity band and related positive parity ones have been determined from lifetimes measured in the present experiment. Extracted $B(E2)$ s and $B(E1)$ s provide important information to probe the remnant of clustering in ^{35}Cl . Large basis shell model (LBSM) calculations have been done to understand the evolution of collectivity along this band. The predicted [4] negative parity partner band of

the SD band in ^{36}Ar has also been reproduced within LBSM calculations for the first time. Spectroscopic factors have been used to correlate the SD states in ^{35}Cl to the cluster states in ^{36}Ar to establish the persistence of alpha-clustering features.

High spin states of ^{35}Cl have been populated through $^{12}\text{C}(^{28}\text{Si},\alpha p)^{35}\text{Cl}$ reaction in the inverse kinematics with an 110 MeV ^{28}Si beam at Inter University Accelerator Center (IUAC), New Delhi. The target was ^{12}C ($50 \mu\text{g}/\text{cm}^2$) evaporated on $18 \text{mg}/\text{cm}^2$ Au backing. The γ - γ coincidence measurement has been done using the multi detector array of thirteen Compton suppressed clover detectors (INGA setup). The relevant details of the experimental setup have been discussed in [14]. The detectors were placed at 148° (4), 123° (2), 90° (4), 57° (2) and 32° (1). The experimental data have been sorted into angle dependent symmetric (90° vs 90°) and asymmetric γ - γ matrices to get the information about the gamma intensities, DCO ratios and level lifetimes of this band.

In our earlier work [15], we have discussed about a few totally shifted gamma rays in the spectra emitted from states having lifetimes shorter than the characteristic stopping time ($\simeq 10^{-13}$ s) of ^{35}Cl recoils in gold (Au) backing. Analysis of the present data confirmed [16] that four of them (2912 keV, 1862 keV, 2391 keV and 3734 keV) belong to the same sequence (marked as SD in Fig. 1), which is connected to the other states in ^{35}Cl through 1113, 1336, 2232 and 1693 keV transitions (Fig. 1). The lowest state of this sequence 5408 keV ($11/2^-$) is already known to be connected to the 3163 keV ($7/2^-$) through a strong 2244 keV transition [11]. This sequence from 3163 keV ($7/2^-$) state to 16306 keV ($27/2^-$) has been established as the yrast negative parity band. The three topmost transitions in the band show nearly perfect rotational behaviour by the almost linear increase in angular momentum with gamma - ray energy (rotational frequency) (Fig. 2). The plot shows a sharp break between $15/2^-$ to $19/2^-$ indicating a crossing between two weakly interacting bands of different configurations. The kinematic moment of inertia (KMOI) for the top three transitions in yrast band in ^{35}Cl scaled by the mass factor compares very well with those for SD bands in ^{36}Ar and ^{40}Ca . The average KMOI, $\simeq 8 \hbar^2/\text{MeV}$ also compares well with the newly found candidate SD band in ^{28}Si ($\simeq 6\hbar^2/\text{MeV}$) [6]. More dramatically, the inset of Fig. 2 shows that energies of alternating parity states, $15/2^-$, $17/2^+$, $19/2^-$, $21/2^+$, $23/2^-$ and $27/2^-$ follow a linear relation to the $I(I+1)$ values exhibiting an apparent rotational band structure, which characterises nuclear molecular structure [8].

Lineshapes of all gamma rays in the yrast sequence (except the 2244 keV gamma), along with the 2614 keV gamma ray connecting the $17/2^+$ state to $21/2^+$, have been analysed to determine the lifetimes of the corresponding states. Due to the large recoil velocity in inverse kinematics and high energies of the relevant gam-

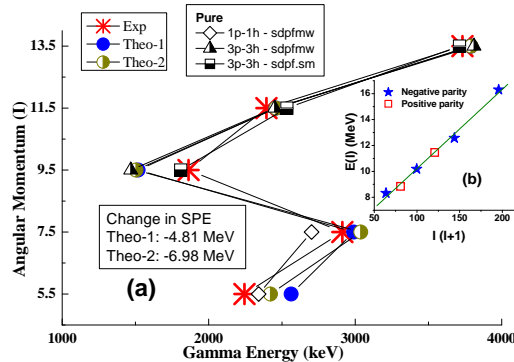


FIG. 2: (a) Comparison of experimental and theoretical backbending plots for the yrast negative parity band in ^{35}Cl . The figure shows the results of calculations with fixed $n\hbar\omega$ and mixed $n\hbar\omega$ truncations viz., Theo1: $[(1d_{5/2})^{12}(2s_{1/2}1d_{3/2})^6(pf)^1 \oplus (1d_{5/2})^{12}(2s_{1/2}1d_{3/2})^4(pf)^3]$; Theo2: $[(sd)^{18}(pf)^1 \oplus (1d_{5/2})^{12}(2s_{1/2}1d_{3/2})^4(pf)^3]$. The amount of depression of the single particle energies (SPE) of pf orbitals in each truncation scheme is also mentioned. (b) The energies ($E(I)$) of $15/2^-$, $17/2^+$, $19/2^-$, $21/2^+$, $23/2^-$ and $27/2^-$ states are plotted as function of $I(I+1)$

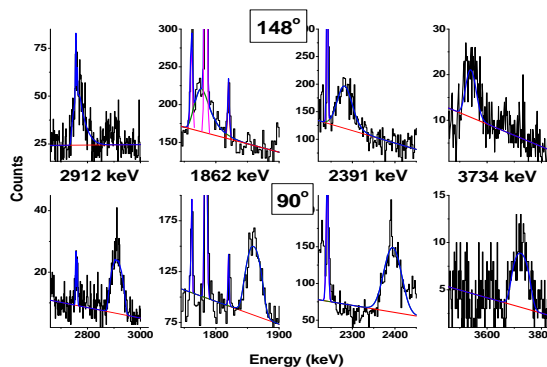


FIG. 3: The Doppler-shift attenuation lineshape analyses for different relevant gamma rays.

mas, special care has been taken to choose the gating transitions such that the slow feeding components are eliminated. Gating from top could not be done due to poor statistics. However, while choosing a suitable gating transition from below, special care has been taken to eliminate the contribution of strong gamma peaks close to the peaks of interest. The spectra at mean angles of 148° and 90° relative to the beam axis were simultaneously fitted (Fig 3) using a modified version of the LINE-SHAPE [18, 19] code which included corrections for the broad initial recoil momentum distribution produced by the α -particle evaporation. The initial momentum distribution of ^{35}Cl recoils has been obtained from statistical model code PACE4 [20]. Lineshapes of four gamma transitions (3734, 2391, 1862 and 2912 keV) were fitted simultaneously as members of a single band. The rotational cascade side-feeding has been considered, assuming 100% side feeding into the top of the band. During each line shape simulation, the background parameters, intensities

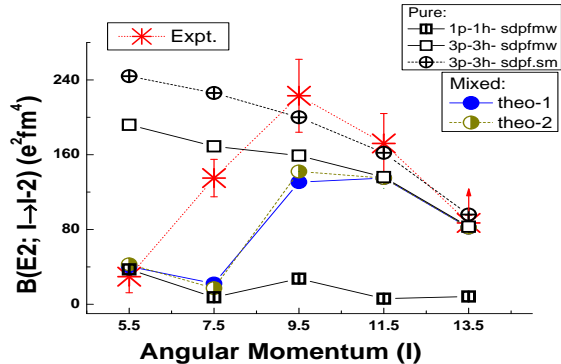


FIG. 4: $B(E2; I_i \rightarrow I_f)$ values for the yrast band in ^{35}Cl compared with the results of shell model calculations.

of the contaminant peaks, and side-feeding quadrupole moments were allowed to vary, and the best fit set was obtained by using the χ^2 minimization. The lineshape of the 1336 keV transition has also been fitted to get an independent estimate of the lifetime of the 10181 keV level. Using the relevant branching ratios [11], experimental B(E2)s were determined from these lifetimes (Fig. 4, Table I). The collectivity in this negative parity band evolves from single particle excitations ($B(E2) \simeq 5$ W.u.) at lower spins, to a set of highly deformed SD states ($B(E2) \simeq 20$ -33 W.u.) in between, finally terminating at a state at $27/2^-$ with moderate deformation ($B(E2) \simeq 13$ W.u.). The gamma transition (2614 keV) connecting the positive parity states also has comparable B(E2) ($\simeq 16$ W.u.). The decay-out transitions (1336 keV and 1113 keV) have relatively large B(E1) values, *viz.*, 2.9 and 2.6×10^{-3} W.u., respectively. In ^{36}Ar and ^{40}Ca , with 4p-4h and 8p-8h excitations in the pf ($N=3$) shell, the deformation (β_2) in the SD bands were 0.45 [2] and $\simeq 0.59$ [1], respectively. In ^{35}Cl , 3p-3h excitations (discussed below) give rise to SD structure with comparable KMOI but relatively smaller deformation ($\simeq 0.37$) (Table I) similar to the observation in heavier nuclei where the occupation numbers of high-N orbitals have been found to characterise SD bands.

Large basis shell model (LBSM) calculations have been done using the SDPFMW Hamiltonian [22] (as referred to within the OXBASH code package [23]). The SDPF.SM [1–3] Hamiltonian suitable for fixed $n\hbar\omega$ [3] excitation has also been used. The valence space consists of full $sd-pf$ orbitals for both protons and neutrons above the ^{16}O inert core (see Ref. [15] for details). The negative (positive) parity spectra have been calculated with pure $\hbar\omega = 1$ (0) and 3 (2) excitations (Fig. 2). The experimental gamma energies ($E_\gamma = E(I) - E(I-2)$) and corresponding B(E2)s for lowest state ($I=11/2^-$) and the upper three states ($I=19/2^-$ to $27/2^-$) agree reasonably well with the calculated values with 1p-1h and 3p-3h excitations, respectively. The results with SDPF.SM exhibit better agreement with the experimental data for spins

TABLE I: Experimental level lifetimes, experimental and theoretical (Theo2) reduced transition probabilities ($B(L)$) for different transitions, corresponding transition quadrupole moments, Q_t (eb), together with quadrupole deformation (β_2) and X (major to minor axis ratio of an ellipsoid) deduced [21] from Q_t s are tabulated. The units of B(E1), B(E2) and B(M1) are $10^{-3}e^2fm^2$, e^2fm^4 and $10^{-2}\mu_N^2$, respectively. The effective charges are $e_p = 1.5e$, $e_n = 0.5e$. For B(M1) calculations, free single particle g factors have been used.

I_i^π	τ_{mean} fs	E_γ keV	B(L)		Q_t eb	β_2	X
			Exp.	Theo2			
11/2 ⁻	400(100)	2244 (E2)	29(8)	43	0.31(4)	0.15	1.16
			[17]				
15/2 ⁻	18(1)	2912 (E2)	135(10)	17	0.65(2)	0.30	1.32
		2232(M1)	<10	1.3			
19/2 ⁻	61(4)	1862 (E2)	224(31)	142	0.82(6)	0.37	1.41
		61(7)	1336 (E1)	1.98(2)	1.03		
			1693 (E2)	148(41)	15		
23/2 ⁻	48(6)	2391 (E2)	172(22)	135	0.71(5)	0.32	1.35
			1113 (E1)	1.8(2)	1.22		
27/2 ⁻	< 13	3734 (E2)	> 87	82	>0.5	0.24	1.25
21/2 ⁺	62(3)	2614 (E2)	108(5)	67	0.56(2)	0.27	1.28

TABLE II: Comparison between wavefunctions of different states obtained from empirical fit and theoretical calculations. The 3p-3h components can be determined from normalisation condition.

E_x	I_i	E_γ^{decay}	Wavefunction (1p-1h)		
			Emp.	Theo1	Theo2
10181	19/2 ₁	1862	0	-	0
8319	15/2 ₁	2912	9	13	8
5408	11/2 ₁	2244	16	68	76
3163	7/2 ₁	3163	94	75	80

19/2⁻ to 27/2⁻ (Figs. 2, 4). However, for $I=15/2^-$, although the gamma energy agrees well with 1p-1h results, the experimental B(E2) matches better to the theoretical B(E2) values from 3p-3h calculations (Fig.4). The reduction in experimental B(E2) at 27/2⁻ is reproduced well by theory. This decrease indicates band termination at 27/2⁻, consistent with a proton hole coupled to the terminating spin (16^+) in the superdeformed band in ^{36}Ar nucleus [2, 3].

Configuration mixing between 1p-1h, 3p-3h configurations has been included for further improvement of the results. The set Theo1 has inert $1d_{5/2}$ in 1p-1h excitation, whereas in Theo2, this orbital was active (Fig. 2). Inclusion of 5p-5h configurations has been found to be insignificant. It has been shown earlier that to reproduce the experimental data, the $sd-pf$ shell gap has to be decreased depending upon the particular truncation scheme involved [15, 24]. In the experimental spectra (Fig.1), two close lying 15/2⁻ states (energy difference is

$\simeq 169$ keV) are seen. The single particle energies (SPE) of the pf orbitals have been shifted downwards to reproduce the splitting between the two lowest $15/2^-$ states. Results from mixed calculations show improvement in reproducing the gamma energy of $15/2^-$ state (Fig. 2) deteriorating the agreement for $B(E2; 15/2^- \rightarrow 11/2^-)$ value. The reduced transition probabilities of decay-out E1 transitions (1336, 1113 keV) are reproduced well (Table I). Shell model calculations reproduce the transition energy and $B(E2)$ of the 2614 keV transition reasonably well. The highest limit of experimental $B(M1)$ for 2232 keV transition is larger than the predicted value. However, the calculated values of $B(E2; 19/2_1^- \rightarrow 15/2_2^-)$ (1693 keV) and $B(E2; 15/2_1^- \rightarrow 11/2_1^-)$ (2912 keV) both are severely underpredicted (Table I), indicating inadequacy of the configuration mixed calculations. In ^{36}Ar , ^{40}Ca also [2, 3], the calculations failed to reproduce the transition probabilities for the states where different configurations interact to their maximum.

A simple phenomenological approach [25] using two level mixing between pure $3p$ - $3h$ and $1p$ - $1h$ states have been used to determine the extent of configuration mixing existing in the states near the band crossing. In this calculation the $19/2^-$ state has been assumed to be a $3p$ - $3h$ state (100%) with no mixing from $1p$ - $1h$ (0%). Utilising the transition matrix elements from pure $1p$ - $1h$ and $3p$ - $3h$ LBSM calculations, the experimentally observed $B(E2; I \rightarrow I-2)$ values for the transitions with $I < 19/2^-$ have been reproduced considering the the mixing coefficients of two component wavefunction for each state as variables (Table II). The shell model predictions deviate from the phenomenologically determined wavefunction structure only for the $11/2^-$ state. It is evident that this deviation leads to the large difference between the experimental and predicted (Theo1 and Theo2) $B(E2)$ for the $15/2^- \rightarrow 11/2^-$ transition.

The SD band in ^{36}Ar has been shown to originate from the band crossing of $(^{32}\text{S}(I^\pi = 0^+ - 8^+) + \alpha)$ cluster bands [4]. The existence of a negative-parity partner band of the SD band is also predicted [4]. Even in shell model picture, a negative parity partner of the SD band in ^{36}Ar has been obtained in terms of $3p$ - $3h$ excitation $((sd)^{17}(pf)^3)$ in the pf shell. So far, it has not been verified experimentally. The parentage of the negative parity SD states in ^{35}Cl in terms of a proton hole coupled to the alpha cluster SD states in ^{36}Ar core, have been obtained from calculated spectroscopic factors (Theo1) (Fig. 5). The $15/2^-$ to $27/2^-$ states in ^{35}Cl are generated primarily from the cluster SD states, 10^+ to 16^+ , whereas, the $17/2^+$ and $21/2^+$ arise predominantly from the 11^- and 13^- states in the negative parity partner band in ^{36}Ar . The observed $17/2^+$ and $21/2^+$ states in ^{35}Cl therefore provide indirect experimental evidence in favour of the existence of a negative-parity partner band of the SD band in ^{36}Ar as predicted in Ref [4] and present work.

Using the weak coupling model [10], the interaction

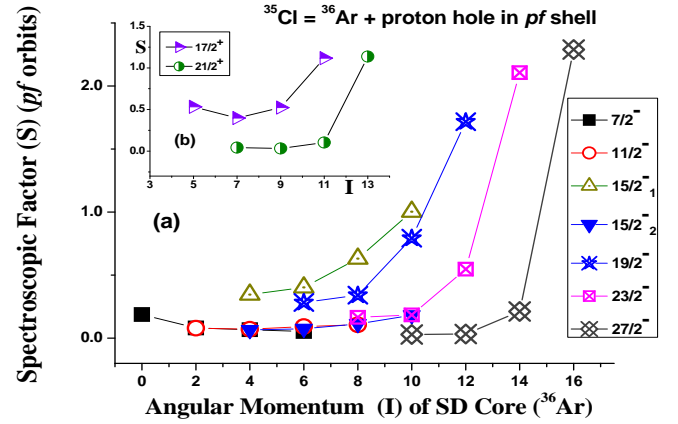


FIG. 5: Calculated spectroscopic factors (Theo1) for the (a) negative parity odd-spin SD states in ^{35}Cl and (b) positive parity partner even spin states to estimate the contribution of the positive parity SD states and their negative parity partners of the core nucleus, ^{36}Ar .

energy of (SD states in $^{36}\text{Ar} + \pi 1f_{7/2}$ hole) which gives rise to the SD states in ^{35}Cl has been calculated. The $E(\pi 1f_{7/2})_{hole}$ has been estimated from the excitation energy of the $7/2^-$ state in ^{35}Cl at 3163 keV. For example, $V_{int}(15/2^- \text{ in } ^{35}\text{Cl}) = [\{BE(10^+ \text{ SD in } ^{36}\text{Ar}) - E(\text{hole in } 1f_{7/2})\} - BE(15/2^- \text{ SD in } ^{35}\text{Cl})]$ These estimations show that to generate $15/2^-$ to $27/2^-$ SD states in ^{35}Cl , by coupling a proton hole with 10^+ to 16^+ SD states in ^{36}Ar , the interaction energies [13] are 915 keV, 175 keV, -382 keV and -714 keV, respectively. These are small compared to a few MeV average particle-particle interaction, and in two of the cases are repulsive, which is favourable for cluster structure formation. The unequal masses of the underlying clusters give rise to dipole degree of freedom leading to the formation of an apparent rotational band containing alternating parity sequence (Fig.2) connected by strong E1 transitions. These E1 transitions are stronger than 2×10^{-3} W.u. indicating that the corresponding positive parity states are doublet partners [8].

To summarize, a superdeformed rotational band with average transition quadrupole moment $Q_t \simeq 0.75$ eb and kinematic moments of inertia $\simeq 8\hbar^2/MeV$ has been identified for the first time in odd ^{35}Cl which terminates at $27/2^-$. The energies of alternating parity states, $15/2^-$, $17/2^+$, $19/2^-$, $21/2^+$, $23/2^-$ and $27/2^-$ connected by strong $B(E1)$ s ($> 2 \times 10^{-3}$ W.u.) and strong cross-over E2 transitions, follow a linear relation to the $I(I+1)$ values providing a strong evidence in favour of cluster structure of these states. Results of LBSM calculations have shown that the SD band has been generated by $3p$ - $3h$ excitations $((sd)^{16}(pf)^3)$ configuration). A simple two level mixing calculation has been done to extract the wavefunction structure of these mixed states from the experimental $B(E2)$ values. Weak coupling estimation in terms of ^{36}Ar and a proton hole clearly identifies the origin of each SD state. The spectroscopic factors are calcu-

lated to estimate parentage of these SD states and their partners in terms of a proton hole coupled to the alpha cluster SD states in ^{36}Ar core. The observed $17/2^+$ and $21/2^+$ states in ^{35}Cl therefore provide indirect experimental evidence in favour of the existence of a negative-parity partner band of the SD band in ^{36}Ar as predicted in Ref [4] and present work.

The authors acknowledge the help from all other INGA collaborators and the Pelletron staff of IUAC for their sincere help and cooperation. Special thank is due to Pradipta Das for his technical help for target preparation. Discussions with P. Banerjee and A K Singh during analysis of the DSAM data are gratefully acknowledged. One of the authors (A.B.) has been financially supported by Council of Scientific and Industrial Research (CSIR), India, under contract No 09/489(0068)/2009-EMR-1.

* corresponding author: maitrayee.sahasarkar@saha.ac.in

- [1] E. Ideguchi, *et al.*, Phys. Rev. Lett. **87**, 222501 (2001); C. J. Chiara *et al.*, Phys. Rev. C **67**, 041303 (R) (2003).
- [2] C. E. Svensson *et al.*, Phys. Rev. Lett. **85**, 2693 (2000); Phys. Rev. C **63**, 061301(R) (2001).
- [3] E. Caurier, F. Nowacki, and A. Poves, Phys. Rev. Lett. **95**, 042502 (2005); E. Caurier, J. Menéndez, F. Nowacki, and A. Poves, Phys. Rev. C **75**, 054317 (2007).
- [4] T. Sakuda, S. Ohkubo, Nucl. Phys. A **744**, 77 (2004).
- [5] J. Cseh, A. Algora, J. Darai, P. O. Hess, Phys. Rev. C **70**, 034311 (2004); Yasutaka Taniguchi, Masaaki Kimura, Yoshiko Kanada-En'yo, and Hisashi Horiuchi, *ibid.* **76**, 044317 (2007).
- [6] D. G. Jenkins *et al.*, Phys. Rev. C **86**, 064308 (2012); J. Darai, J. Cseh and D. G. Jenkins, Phys. Rev. C **86**, 064309 (2012).
- [7] Eric D. Johnson, Ph.D. thesis, Florida State University, 2008 and references therein.
- [8] Y. Alhassid, M. Gai, and G. F. Bertsch, Phys. Rev. Lett. **49**, 1482 (1982); M. Gai, M. Ruscev, D. A. Bromley, and J. W. Olness, Phys. Rev. C **43**, 2127 (1991); S. Courtin, A. Goasduff and F. Haas, arXiv:1303.4252v1 [nucl-ex] 18 Mar 2013 and references therein.
- [9] B. Buck and A. A. Pilt, Nucl. Phys. A **280**, 133 (1977); M. Kimura and N. Furutachi, Phys. Rev. C **83**, 044304 (2011) and references therein.
- [10] Akito Arima and Ikuko Hamamoto, Annu. Rev. Nucl. Sci. **21**, 55 (1971).
- [11] <http://www.nndc.bnl.gov>
- [12] K. Ikeda, N. Takigawa and H. Horiuchi, Prog. Theor. Phys. Suppl. Extra No., 464, (1968).
- [13] Georges Audi and Wang Meng, Private Communication April 2011; G. Audi *et al.*, Chinese Physics C **36**, 1287 (2012).
- [14] S. Muralithar *et al.*, Nucl. Instr. and Meth. A **622** (2010) 281.
- [15] R. Kshetri, *et al.*, Nucl. Phys. A **781** (2007) 277; Abhijit Bisoi *et al.*, Proc. DAE-BRNS Symp. Nucl. Phys. (India) **55**, 4 (2010).
- [16] F. Della Vedova, *et al.*, Phys. Rev. C **75**, 034317 (2007); LNL Annual Report 2004.
- [17] P.R.G. Lornie, *et al.*, J. Phys. A **7**, 1977 (1974).
- [18] J.C. Wells, N.R. Johnson, Report ORNL-6689, 1991, p. 44.
- [19] R.K. Bhowmik, Private Communication.
- [20] A. Gavron, Phys. Rev. C **21**, 230 (1980).
- [21] <http://www.physics.mcmaster.ca/~balraj/sdbook/>
- [22] E.K. Warburton, J.A. Becker, B.A. Brown, Phys. Rev. C **41**, 1147 (1990).
- [23] B.A. Brown, *et al.*, OXBASH for Windows, MSU-NSCL Report. Number 1289, 2004.
- [24] Indrani Ray *et al.*, Phys. Rev. C **76**, 034315 (2007); M. Saha Sarkar, Proc. DAE-BRNS Symp. Nucl. Phys. (India) **55**, 119 (2010); <http://www.symppnp.org/proceedings/index.php>: electronic version only.
- [25] H. T. Fortune, Phys. Rev. C **86**, 024305 (2012).